JOURNAL OF APPLIED ELECTROCHEMISTRY 17 (1987) 1281–1295

Influence of various coated paper separator materials on the corrosion, polarization and impedance characteristics of zinc in concentrated sodium chloride solution

L. M. BAUGH*, N. C. WHITE

Ever Ready Ltd, Technical Division, Tanfield Lea, Stanley, Co. Durham DH9 9QF, UK

Received 11 March 1986; revised 31 March 1987

The corrosion characteristics of amalgamated zinc have been studied in 2.7 M NaCl at pH 4.8 using steady-state polarization and a.c. impedance methods, and the influence of various coated paper separators has been determined. It is shown that the polarization behaviour in either the presence or absence of the separator materials can be interpreted if due consideration is given to diffusion and charge transfer effects. The anodic zinc dissolution process is jointly controlled by these effects whereas the cathodic hydrogen evolution (proton reduction) process is diffusion limited.

Using a simple model which takes into account the quasi-reversible nature of the zinc dissolution process, good agreement between calculated and observed current inhibition factors can be obtained if the surface blocking (coverage) effect of the separators is combined with the effect of the change in diffusion path length through the separator pores. Application of this model to the diffusion-limited hydrogen evolution reaction, however, fails unless the blocking term is ignored.

Nomenclature

A_e	area fraction of electrolyte in contact with the electrode
A_p	area fraction of polymer in contact with the electrode
b_a	anodic slope of semi-logarithmic current–potential plot
b_c	cathodic slope of semi-logarithmic current–potential plot
C	surface concentration of zinc species in the absence of the separator
C_s	surface concentration of zinc species in the presence of the separator
C_b	bulk concentration of protons
C_{dl}	double layer capacity
D	diffusion coefficient in the absence of the separator
D_s	diffusion coefficient in the presence of the separator
i	current in the absence of the separator
i_s	current in the presence of the separator
i_{ct}	charge transfer current
i_d	diffusion current
i_c	cathodic current
i_0	exchange current
i_{cor}	corrosion current
$i_{cor}^{R_{dc}}$	corrosion current derived from R_{dc} value
$i_{cor}^{R_p}$	corrosion current derived from R_p value
i_{cor}^{Ext}	corrosion current derived by extrapolation of polarization curves
i_{cor}^{Bat}	corrosion current estimated in complete battery environment
I_{cor}	corrosion inhibition efficiency (%)
k_f	potential-dependent forward rate constant
k_b	potential-dependent backward rate constant
l	mean pore length
r_e	resistance of free electrolyte having the

* *Present address*: BNF Metals Technology Centre, Grove Laboratories, Denchworth Road, Wantage, Oxon OX12 9BJ, UK.

0021–891X/87 $03.00 + .12

same overall volume and geometry as the separator

r_s resistance of electrolyte within the separator matrix

R_Ω resistance of electrolyte between Luggin reference probe and electrode surface in the absence of the separator

R_Ω^s resistance of electrolyte between Luggin reference probe and electrode surface in the presence of the separator

R_{ct} charge transfer resistance

R_{dc} d.c. resistance

R_p polarization resistance

t thickness of the separator

t_p thickness of the base paper

t_c thickness of the coating layer

V_e volume fraction of electrolyte in the separator

x distance of Luggin reference probe from electrode surface (absence of separator) or electrolyte exposed outer separator surface (presence of the separator)

δ diffusion layer thickness

θ tortuosity factor

Subscripts/superscripts

1,2 separator 1,2

A,B,C separator A,B,C

1. Introduction

In previous investigations the effect of methyl cellulose-coated paper separators on zinc exchange [1] and corrosion reactions [2, 3] was studied in *standard* Leclanché and related electrolyte analogues. The standard electrolyte used in *base* grade batteries consists of a mixture of zinc chloride and ammonium chloride, typically 2 M $ZnCl_2$ + 6 M NH_4Cl. Premium grade cells, however, have an electrolyte which consists either entirely or predominantly of zinc chloride. This change in composition affects the corrosion behaviour of zinc anodes in particular, which is highlighted by carrying out polarization experiments in an analogue electrolyte consisting of pure sodium chloride at the same ionic strength and pH as the battery electrolyte, namely 2.7 M NaCl at pH 4.8 [4]. The absence of zinc ions in the electrolyte formulation prevents interference from zinc deposition which would otherwise dominate during cathodic polarization and obliterate hydrogen evolution characteristics. The present paper is concerned with an assessment of the influence of various coated and uncoated paper separator materials on the corrosion behaviour of zinc in this *premium* grade Leclanché electrolyte analogue.

The overall component reactions which determine the net corrosion process in zinc chloride Leclanché electrolyte can be represented as follows:

$$Zn + nCl^- \rightleftharpoons ZnCl_n^{2-n} + 2e \quad \text{anodic} \quad (1)$$

and

$$2H_2O + 2e \longrightarrow 2OH^- + H_2 \quad \text{cathodic} \quad (2)$$

$$Zn + nCl^- + 2H_2O \longrightarrow ZnCl_n^{2-n} + 2OH^- + H_2 \quad (3)$$

or

$$Zn + nCl^- \rightleftharpoons ZnCl_n^{2-n} + 2e \quad \text{anodic} \quad (4)$$

and

$$2H_3O^+ + 2e \longrightarrow 2H_2O + H_2 \quad \text{cathodic} \quad (5)$$

$$Zn + nCl^- + 2H_3O^+ \longrightarrow ZnCl_n^{2-n} + 2H_2O + H_2 \quad (6)$$

In these reaction sequences the formation of solid products is not considered. The occurrence of reactions 3 or 6 is dependent upon whether the zinc is unamalgamated or amalgamated, respectively [4]. It is clear that any change in the rates of these reactions resulting from the presence of a separator adjacent to the zinc will depend upon the extent to which the material induces changes in the rates of the individual component reactions. This in turn will depend upon their exact mechanisms and the nature of their rate control as well as the chemical identity of the species involved. A detailed

knowledge of these reactions in the absence of the separator is clearly important. In the present paper, polarization and impedance techniques have been applied to the study of both amalgamated and unamalgamated zinc electrodes, although the former have been predominantly studied.

2. Theoretical

2.1. *Zinc dissolution process*

The overall dissolution reaction can be represented by reaction 4, but for convenience we propose to consider the reaction product as $ZnCl_4^{2-}$. Thus the reaction is

$$Zn + 4Cl^- \rightleftharpoons ZnCl_4^{2-} + 2e \tag{7}$$

This quasi-reversible reaction can be treated in the same manner as that for zinc dissolution in concentrated alkaline solution, in which the product is $Zn(OH)_4^{2-}$ and where the current is controlled by combined charge transfer and mass transfer effects [5, 6]. At low to medium current values the equality of charge transfer and diffusion fluxes gives the following expressions for the steady-state condition

$$i = i_{ct} = i_d = nFk_f - nFk_b C = nFDC/\delta \tag{8}$$

It is important to note that C is a dependent variable since it cannot be *directly* controlled and varies in response to the other (independent) variables E, D and δ [6]. In the presence of a separator the latter two parameters are affected and these in turn must also affect C. Values of D must be modified for changes in electrolyte volume fraction, V_e, and tortuosity, θ. Assuming a simple pore model [8]

$$D_s = DV_e/\theta^2 \tag{9}$$

The value of δ can be equated with the thickness, t, of the separator,

$$\delta = t \tag{10}$$

At the same time the charge transfer current must be modified for the blocking effect of the separator on the metal surface using the area fraction of electrolyte adjacent to the zinc, A_e, as the correction factor [1, 2]

$$i_{ct}^s = i_{ct}A_e \tag{11}$$

Substitution of Equations 9 to 11 into Equation 8 gives

$$i_s = A_e(nFk_f - nFk_bC_s) = nFC_sDV_e/\theta^2 t \tag{12}$$

Using a simple model for the pores within the separator as a series of 'hose-pipes' with the current flow at the electrode surface being perpendicular to the plane of the electrode and thereafter parallel to the axes of the pores, the following expression can be derived:

$$V_e = A_e\theta$$

and hence the right hand side of Equation 12 becomes

$$i_s = nFC_sDA_e/\theta t \tag{13}$$

Furthermore, $\theta t = l$, and therefore Equation 13 can be replaced by

$$i_s = nFC_sDA_e/l \tag{14}$$

Equation 14 shows that the current in the presence of the separator is directly proportional to the area fraction of electrolyte adjacent to the metal and inversely proportional to the path length for diffusion.

Assuming $C_s \approx C$, which is a reasonably good approximation for variations in diffusion layer thickness much less than an order of magnitude, two useful relationships can be derived from

Equations 8 and 12–14. Firstly, the current ratio in the presence and absence of the separator is given by

$$i_s/i = V_e\delta/\theta^2 t = A_e\delta/\theta t = A_e\delta/l \quad (15)$$

Secondly, for two different separators the current ratio is

$$i_{s,1}/i_{s,2} = V_{e,1}\theta_2 t_2/V_{e,2}\theta_1 t_1 = A_{e,1}\theta_2 t_2/A_{e,2}\theta_1 t_1 = A_{e,1}l_2/A_{e,2}l_1 \quad (16)$$

A knowledge of the separator parameters on the right hand side of Equations 15 and 16 allow the respectively current ratios to be calculated. These calculated values can be compared with the experimentally derived ratios which are directly accessible from polarization curves.

2.2. *Hydrogen evolution process*

The hydrogen evolution reaction which is relevant to most of the experiments conducted in the present investigation is reaction 5. This is diffusion-limited [4, 5] and the expression for the current in the absence of the separator is

$$i = nFC_b D/\delta \quad (17)$$

In the presence of a separator the modified expression is

$$i_s = nFC_b D_s/t = nFC_b DV_e/\theta^2 t \quad (18)$$

$$= nFC_b DA_e/\theta t \quad (19)$$

$$= nFC_b DA_e/l \quad (20)$$

The expressions for i_s/i and $i_{s,1}/i_{s,2}$ are identical to Equations 15 and 16.

3. Experimental details

The electrode preparation, electrochemical cell, electrode assemblies, instrumentation and experimental procedure have been described previously [7]. The technique for determining separator resistances, tortuosities and volume fractions from ohmic impedance data has also been described [2], together with the method of amalgamation [1]. The electrolyte was 2.7 M NaCl at pH 4.8 and the reference electrode was $Hg/Hg_2Cl_2/KCl$ (sat) for experiments in flooded electrolyte.

Four different separator papers were investigated. Coated separators contained calomel at the level of $1.6\,g\,m^{-2}$.

(i) Separator A: an uncoated, unbleached absorbent α-cellulose paper of $75\,g\,m^{-2}$ and thickness 140 μm.

(ii) Separator B: essentially a $30\,g\,m^{-2}$ coating of Starch and Karaya Gum (2.5 : 1), 41 μm thick, on separator A.

(iii) Separator C: a $16\,g\,m^{-2}$ double-sided coating of a highly cross-linked starch and polymeric binder, 22 μm thick, on unbleached absorbent α-cellulose paper of $64\,g\,m^{-2}$ and thickness 92 μm.

(iv) Separator D: a $30\,g\,m^{-2}$ coating of methylcellulose, 30 μm thick, on bleached absorbent α-cellulose paper of $100\,g\,m^{-2}$ and thickness 185 μm. This separator was used in previous investigations [1–3].

4. Results and discussion

4.1. *Polarization and impedance characteristics*

Fig. 1 shows the effect of amalgamation on the polarization and impedance characteristics of zinc in the absence of a separator. The extreme differences are due primarily to the presence of an oxide

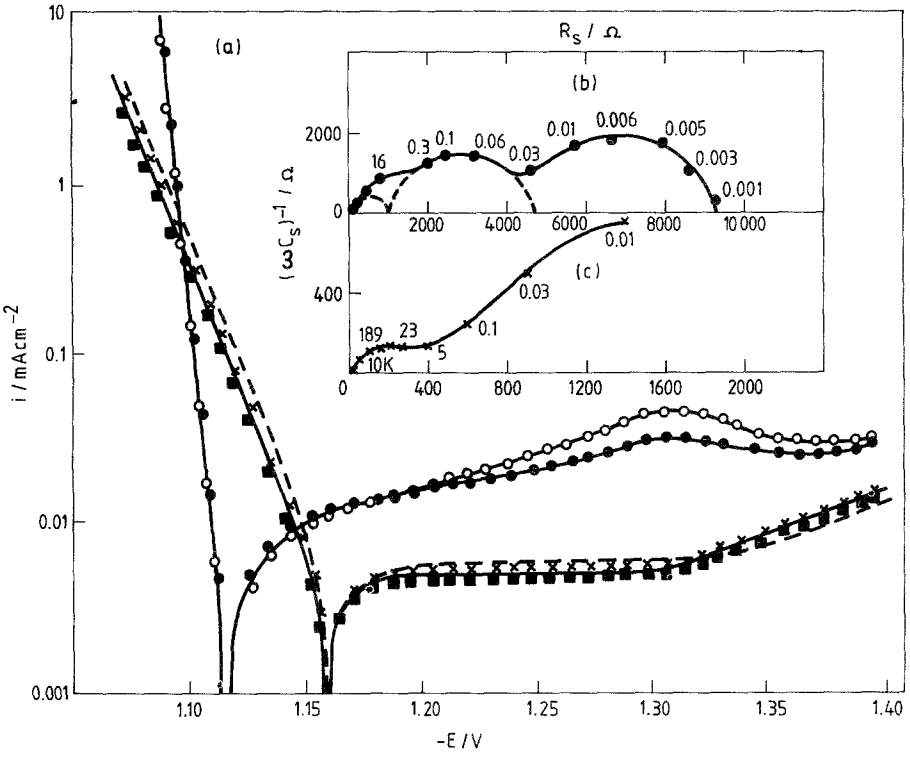

Fig. 1. (a) Polarization characteristics and (b, c) impedance spectra at the rest potential (frequency range 50 kHz–3 mHz) for zinc in 2.7 M NaCl at pH 4.8, (●○) unamalgamated zinc, (×■) amalgamated zinc; (– – –) curves obtained in previous work using controlled cathodic electrodeposition method of amalgamation.

film on the unamalgamated zinc surface [4, 7]. This causes the slope of the anodic polarization line to deviate appreciably from the 30 mV per decade value expected for a film-free surface upon which reversible dissolution–deposition of zinc occurs. The cathodic branches of the polarization curves also show significant differences. In the case of unamalgamated zinc at low potentials a pseudo-Tafel line of high slope appears, followed by a reduction peak at -1.30 V. Thus, initially, the cathodic process is hydrogen evolution via water reduction (reaction 2) which occurs directly on the oxide, followed at higher potentials by reaction 2 occurring on the base metal. In the case of amalgamated zinc at low potentials a diffusion-limited current is observed which can be attributed to proton reduction (reaction 5). However, at higher potentials (< -1.30 V) the predominant process changes to water reduction when the rate of reaction 2 is sufficiently enhanced by the applied potential. In the previous study, amalgamation was achieved by controlled cathodic deposition of mercury from HgO-saturated KOH solutions [4]. This is in contrast with the method employed in the present work which involves mercury deposition from Hg_2Cl_2 (in the separator coating) via zinc displacement at the open-circuit potential. The agreement between the present results and those obtained previously (dotted line in Fig. 1a) demonstrates that the method of amalgamation has no influence on the polarization characteristics.

In common with the polarization curves, the impedance spectra for amalgamated and unamalgamated zinc also show quite severe differences. On unamalgamated zinc two processes are distinguishable at high frequencies followed at lower frequencies by a shape which is consistent with a rapidly collapsing Warburg impedance. The complex high-frequency impedance and the relatively small contribution from diffusion to the overall impedance characteristics are symptomatic of the presence of the oxide film. This contrasts with the impedance for amalgamated zinc which is much

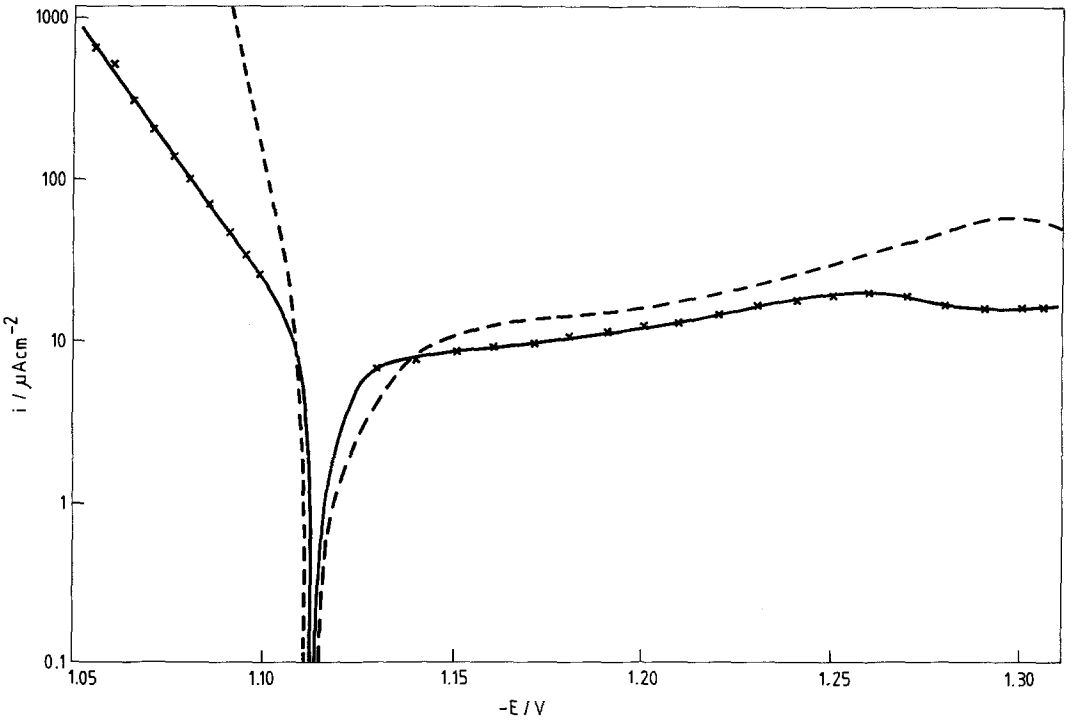

Fig. 2. Effect of separator A on the polarization characteristics of unamalgamated zinc in 2.7 M NaCl at pH 4.8; (– – –) absence of the separator; (×) presence of the separator.

more ideal, consisting of a single charge transfer resistance at high frequencies, followed by a well-defined Warburg impedance at low frequencies.

Fig. 2 illustrates the influence of uncoated separator A on the polarization curves for unamalgamated zinc. The presence of the paper causes a 50 mV anodic shift in the position of the reduction peak and a slight inhibition of the water reduction reaction overall. During anodic polarization, however, the inhibition is more severe primarily as a result of a change in slope of the anodic line. These results can be interpeted if it is assumed that the presence of the separator causes a decrease in the local pH close to the electrode surface. This can occur as a result of the local corrosion-induced rise in zinc chloride concentration [9] which is facilitated by the reduction in convection close to the electrode. This small pH decrease is sufficient to produce a less compact or thinner oxide which is consequently more easily reduced, thus explaining the small shift in cathodic reduction potential. During anodic polarization when the surface concentration of zinc chloride rises more appreciably, the fall in surface pH is more significant resulting in a complete *activation* of the electrode due to film removal. The 30 mV per decade anodic slope proves that the electrode is film-free in the presence of the separator paper.

These interesting, though somewhat unexpected, results highlight the complexity of the NaCl analogue and contrast with those obtained in the case of the standard NH_4Cl analogue [2] where effects due to oxide films are absent. Therefore, in order to aid a basic understanding in these preliminary investigations further work was conducted only with amalgamated zinc upon which it can be assumed no oxide–hydroxide film is present at the pH of relevance, thus eliminating interference from oxide formation–removal effects.

Fig. 3a shows the effect of separators B and C on the polarization curves for amalgamated zinc, and Fig. 3b and c depict the impedance curves for amalgamated zinc in the presence of these separators. Clearly, in contrast with the polarization data in Fig. 2, the effect of the separator is now

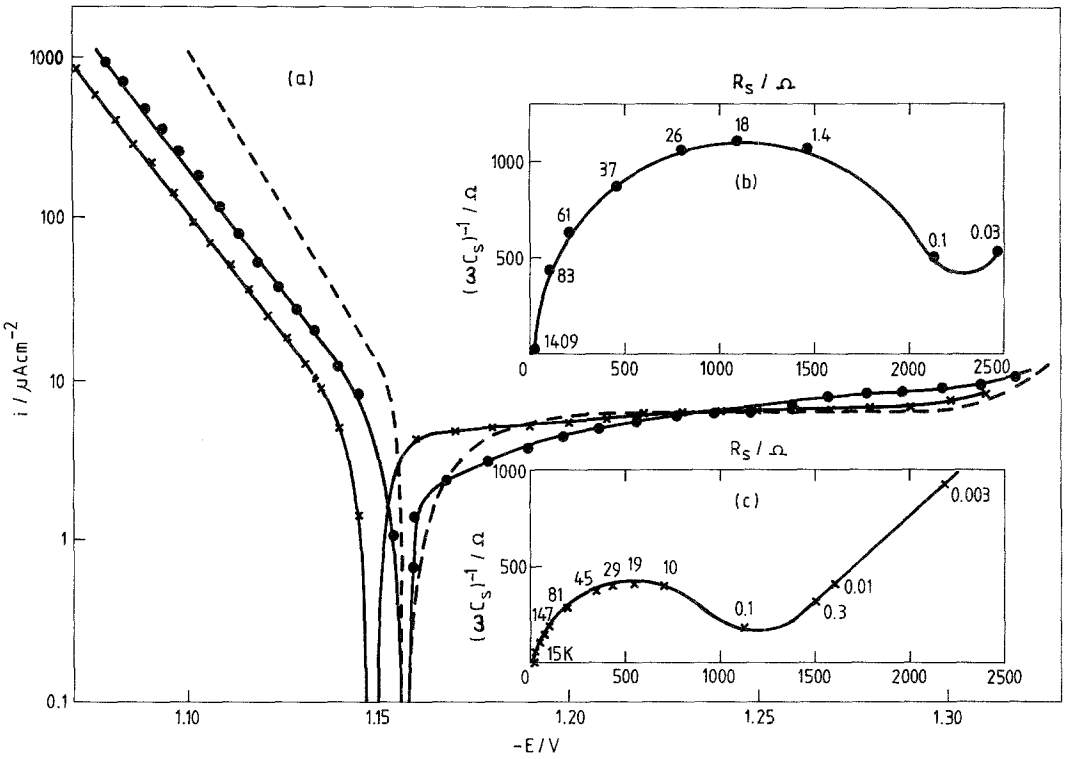

Fig. 3. (a) Polarization characteristics and (b, c) impedance spectra at the rest potential (frequency range 50 kHz–3 mHz) for amalgamated zinc in 2.7 M NaCl at pH 4.8; (– – –) absence of a separator; (×) presence of separator B; (●) presence of separator C.

one of degree rather than kind. The anodic polarization line is shifted in the positive direction almost parallel to the base line, the effect of separator B being greater than separator C. This difference between the two separators correlates qualitatively with the increase in thickness of the base paper, $\Delta t = 48\,\mu$m, since the overall coating thicknesses are about equal (41–44 μm). In the absence of significant differences in tortuosity or volume fraction, the major difference in current is caused by the change in diffusion layer thickness (see Section 2). The thicker separator decreases the rate of diffusion of zinc species leaving the vicinity of the electrode surface at any potential value relative to that for the thinner material. The diffusion flux consequently decreases. This in turn causes a small rise in the surface concentration of dissolving zinc species and therefore a greater deposition current. As a result the charge transfer flux falls in parallel with the change in diffusion flux and hence the net current also falls (see Equation 12). The presence of large charge transfer semicircles in the impedance diagrams of Fig. 3b and 3c proves the quasi-reversible nature of the dissolution reaction upon which Equation 12 depends.

In contrast with the significant inhibition of the anodic process discussed above, the cathodic reaction is little affected, particularly at higher potentials. In the case of separator B a truly limiting current is observed which is identical to that for the base metal. This result is difficult to reconcile with the anodic behaviour. An attempt will be made to discuss the influence of the separators in more quantitative terms later in the paper. Nevertheless, at this stage, one of the theoretical assumptions made earlier concerning the magnitude of the diffusion layer thickness in the presence of the separator, $\delta = t$, will be considered in more detail. Fig. 4 shows the relationship between cathodic current at -1.250 V as a function of electrode rotation speed ($\omega^{1/2}$) in the presence and absence of separator. In contrast to the behaviour in the absence of the separator, where the current varies with $\omega^{1/2}$ in the manner expected theoretically (particularly at the lower rotation speeds), there

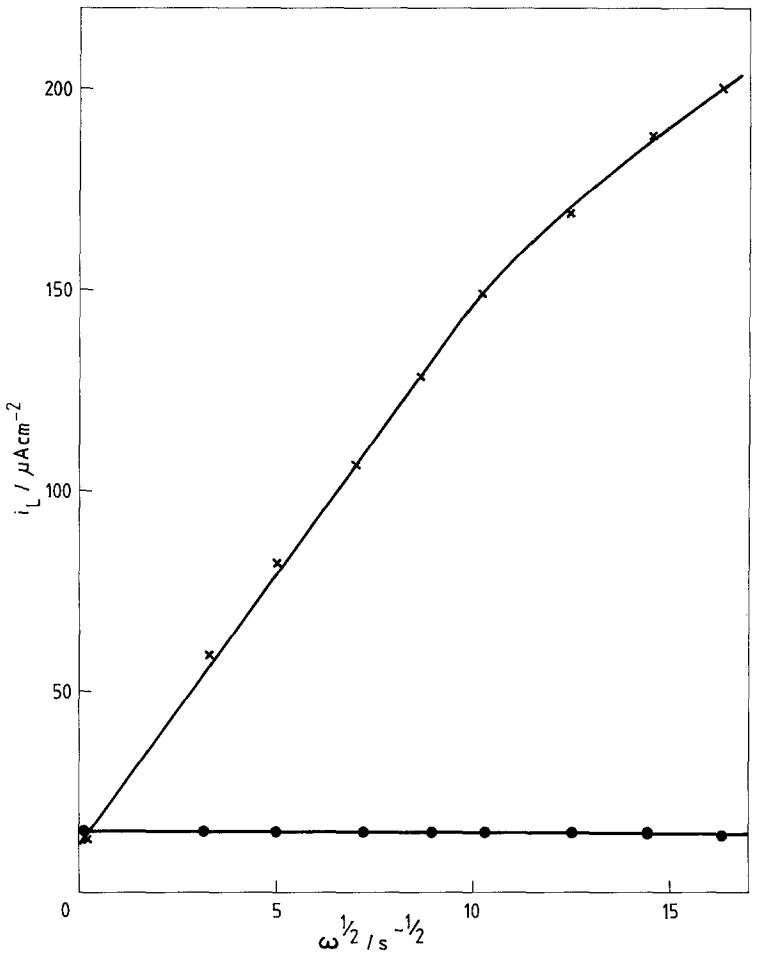

Fig. 4. Effect of electrode rotation speed on the diffusion-limited hydrogen evolution current for amalgamated zinc in 2.7 M NaCl at pH 4.8 ($E = -1.25$ V); (×) absence of the separator; (○) presence of separator B.

is no dependence of the current on ω in the case of the separator covered electrode. This experiment proves conclusively that the diffusion layer thickness in the latter case can be identified with the thickness of the separator.

The impedance characteristics observed at the open-circuit potential (Fig. 3b and 3c) are qualitatively identical and have been drawn on the same scale to accentuate quantitative differences. They can be compared directly with Fig. 1c for amalgamated zinc in the absence of a separator. All the impedance characteristics can be correlated with the overall corrosion process represented by reaction 6, which in turn depends upon the individual component reactions 4 and 5. In the case of amalgamated zinc in the presence and absence of separator B, the hydrogen evolution process is diffusion-limited and therefore cannot respond to the a.c. potential perturbation. It can then be assumed that the impedance spectra reflect those of the metal dissolution component (reaction 4) only. The high-frequency charge transfer resistance can then be identified with the *exchange* current for the reversible zinc dissolution–deposition reaction.

$$i_0 = RT/2FR_{ct} \tag{21}$$

However, the *corrosion* current given by

$$i_{cor} = (1/R_{dc})[b_a b_c/(b_a + b_c)] \tag{22}$$

cannot be determined from the impedance diagrams because $R_{dc} = (Z)_{\omega=0}$ is clearly unobtainable

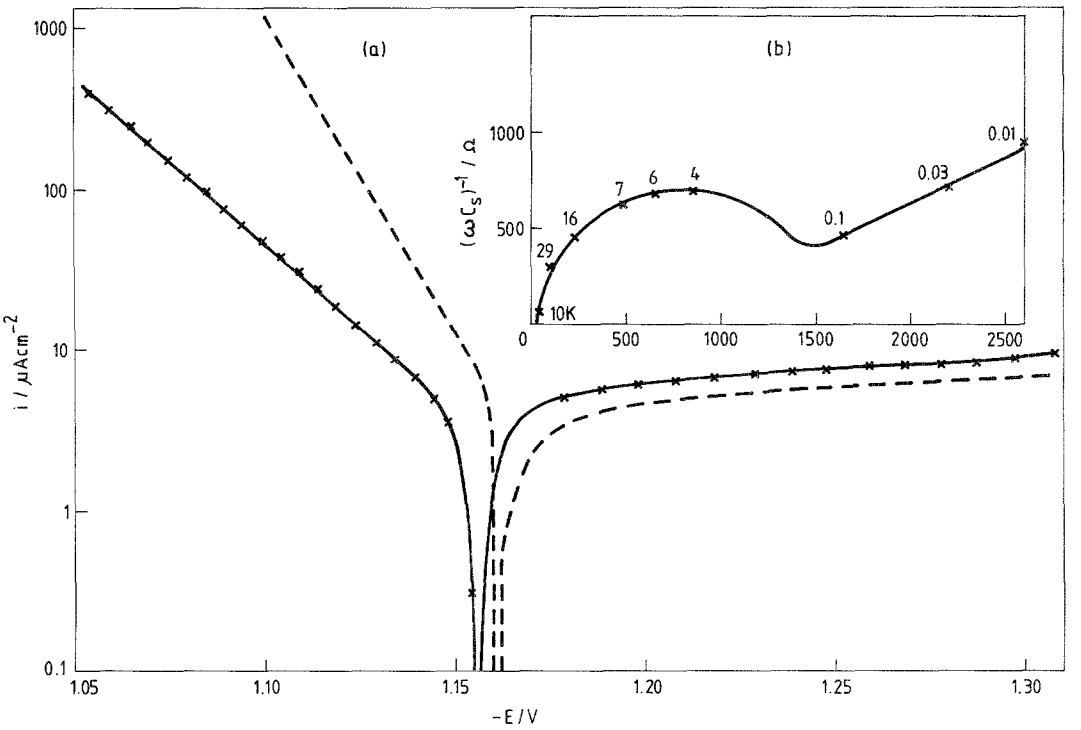

Fig. 5. (a) Polarization characteristics and (b) impedance spectrum (frequency range 50 kHz–3 mHz) for amalgamated zinc in 2.7 M NaCl at pH 4.8; (---) absence of the separator; (×) presence of separator D.

from the usual low-frequency extrapolation method. These results contrast with those obtained for the NH_4Cl analogue [2] and stem from an increase in the importance of diffusion as the process which influences most directly the rate of the joint charge transfer and diffusion-controlled zinc dissolution reaction. (This is also a statement of the fact that there must be 'degrees' of quasi-reversibility with the NaCl case being more reversible than the NH_4Cl case). They indicate that the corrosion current can only be obtained from the steady-state polarization data. In the case of separator C it is clear from Fig. 3a that the hydrogen evolution reaction is not truly diffusion-limited and, in principle, impedance features characteristic of this reaction should also be detectable if present. The qualitative similarity between Fig. 3b and the other impedance diagrams, however, shows that in practice this is not so.

Fig. 5a compares the polarization curves for amalgamated zinc in the presence and absence of separator D and Fig. 5b shows the impedance diagram at the open-circuit potential in the presence of the separator. This methylcellulose-coated material is similar to the separator used in standard Leclanché cells containing NH_4Cl and has been extensively studied in the previous investigations [1–3]. It is clear that whilst the cathodic branches of the polarization curves are very similar, a severe diminution in the anodic current is observed. Furthermore, the slope of the anodic branch is increased from 30 to 45 mV per decade. It is tempting to use a similar argument to that proposed in the case of the zinc–methylcellulose–paper–NH_4Cl system to explain this result; that is, the severe inhibition of the zinc dissolution process causes a change in the nature of rate control from predominantly diffusion control to charge transfer control. However, the impedance spectrum in Fig. 5b shows the presence of a Warburg impedance at low frequencies which cannot be attributed to the hydrogen evolution reaction. Hence, the diffusion process must be ascribed to zinc dissolution, thereby discounting the possibility of charge transfer control. The behaviour of separator D is therefore anomalous. Careful inspection of the slope of the Warburg impedance shows it to be

Table 1. Parameters derived from ohmic impedance data

Electrode–separator system	R_Ω (Ωcm^2)	R^s_Ω (Ωcm^2)	r_e (Ωcm^2)	r_s (Ωcm^2)	r_s/r_e	V_e	θ	A_e	A_p
Zn–separator A	0.28	0.79	0.039	0.51	13.1	0.42	2.4	0.18	0.82
Zn(Hg)–separator B	0.30	1.10	0.054	0.80	14.8	0.41	2.4	0.17	0.83
(Coating only)	(0.30)	(1.10)	(0.012)	(0.29)	(24.2)	(0.35)	(2.9)	(0.12)	(0.88)
Zn(Hg)–separator C	0.30	0.81	0.041	0.51	12.4	0.43	2.3	0.19	0.81

Additional parameters used in calculations: $x = 0.10$ cm; separator A, $t_p = 140\,\mu$m; separator B, $t_p = 140\,\mu$m, $t_c = 41\,\mu$m; separator C, $t_p = 92\,\mu$m, $t_c = 22\,\mu$m (both sides).
NB. V_e, θ and A values for separators B and C are 'effective' values for *complete* separator (base paper + coating layer) except where stated otherwise.

closer to 22° rather than the usual 45°. The former slope is characteristic of either porous electrode behaviour or indicative of surface roughness. It is possible that in view of the very high surface coverage of this separator (approximately 90%) a situation equivalent to gross surface roughness on a separator *free* surface pertains. However, this speculative suggestion requires further confirmation.

4.2. *Separator parameters and quantitative correlation with polarization data*

4.2.1. Zinc dissolution process. Table 1 summarizes the separator parameters derived from ohmic (high-frequency) impedance data. In the case of separator B, 'effective' data in respect of the separator as a whole (base paper + coating layer) is quoted in addition to data specific to the coating layer alone (bracketed). The separation of these data requires a knowledge of the resistance of the base paper [2]. This was available, since separator A is the base paper for separator B. In the case of separator C, however, experiments on the base paper alone were not carried out and hence the quoted parameters are 'averaged' values for the separator as a whole. It must be re-emphasized that the validity of the quoted V_e, θ and A values depends upon the applicability of the pore model [10] which has not been proved in the present work, but which has been shown to be relevant, at least for the base paper, in earlier investigations [1, 2, 11].

It can be seen from Table 1 that the area fraction, A_p, for the base paper A is high at 0.82 or 82% coverage. This is somewhat greater than the value deduced earlier of 65–67% for *bleached* absorbent paper. The tortuosity is also greater at 2.4 compared with 1.7 for the bleached analogue. Addition of the Starch–Karaya Gum coating does not affect the averaged V_e, θ and A values to any significant extent. However, when only the coating layer is considered it has a volume fraction of 0.35 compared with 0.42 for the base paper and a tortuosity of 2.9 compared with 2.4 for the base paper. An area fraction of 0.88 or 88% coverage is also deduced for the coating layer. Separator C has averaged V_e and θ values which are almost identical to those of separators A and B. It may be concluded that the base papers for separators B and C have a very similar composition and structure.

Using the data in Table 1 it is possible to calculate values for the current ratios i_s/i and $i_{s,1}/i_{s,2}$ from Equations 15 and 16, respectively. Three ratios were calculated: i^B/i, i^C/i and i^C/i^B where the superscripts refer to separators B and C. Table 2 compares the experimentally determined ratios with the calculated values. Only the averaged separator parameters in Table 1 have been used in the calculations. In order to calculate the i_s/i values a value for δ, the diffusion layer thickness in the absence of the separator, was required. This is not a constant and obviously depends upon the extent of convection. A value of $\delta = 300\,\mu$m has been used which is not unreasonable. (Choice of a value for δ does not influence the calculated ratio i^C/i^B.) It can be concluded from Table 2 that the agreement between the current ratios is reasonable considering the approximations, not only in the

Table 2. Parameters derived from high current polarization data

Electrode–separator system	*Anodic*						
	b_a *(mV)*	i *($\mu A\,cm^{-2}$)*	i_s *($\mu A\,cm^{-2}$)*	i_s/i		i_i^C/i_s^B	
				Measured	*Calculated*	*Measured*	*Calculated*
Zn(Hg)–separator B	30	750	82	0.11	0.14	2.0	1.5
Zn(Hg)–separator C	30	750	165	0.22	0.21		
	Cathodic						
	b_c *(mV)*	i *($\mu A\,cm^{-2}$)*	i_s *($\mu A\,cm^{-2}$)*	i_s/i		i_s^C/i_s^B	
				Measured	*Calculated*	*Measured*	*Calculated*
Zn(Hg)–separator B	∞	5.0	4.2	0.84	0.81	1.31	1.39
Zn(Hg)–separator C	∞	5.0	5.5	1.10	1.12		

$E_A = -1.050$ V.

theory relating V_e and θ to the current, but also in the theory relating V_e to θ. The experimental determination of the relevant resistance values would also seem to be vindicated. It should also be pointed out that even in the absence of these approximations an *exact* agreement between theory and practice might not be expected in view of possible *specific* effects of the separator coating which cannot be taken into account within the context of present understanding. Some of these effects have been discussed previously in relation to the influence of methylcellulose-coated separators on the zinc exchange reaction in Leclanché electrolyte [1].

4.2.2. Hydrogen evolution process. Although the cathodic currents depicted in Fig. 3 are only truly limiting in the absence of the separators, the current in the presence of separator **B** is almost limiting at low potentials and that for separator C approaches a limiting value at higher potentials. Relationships 15 and 16 should therefore pertain. The near coincidence of the cathodic curves particularly at the higher potentials, however, proves conclusively that this is not the case. Modification of these basic equations is necessary. In their simplest form Equations 15 and 16 can be represented by two terms in brackets,

$$i_s/i = (A_e)(\delta/l) \tag{23}$$

and

$$i_{s,1}/i_{s,2} = (A_{e,1}/A_{e,2})(l_2/l_1) \tag{24}$$

Thus, two effects determine the magnitude of the current ratios. Firstly, a surface blocking (or obstacle) effect and secondly a diffusion path length effect. If it is assumed that in the case of the diffusion-limited hydrogen evolution process studied here the surface blocking effect is absent, then $A_e = A_{e,1} = A_{e,2} = 1$ and Equations 23 and 24 become

$$i_s/i = \delta/l = \delta/\theta t \tag{25}$$

and

$$i_{s,1}/i_{s,2} = l_2/l_1 = \theta_2 t_2/\theta_1 t_1 \tag{26}$$

In order to test this hypothesis, diffusion-limiting currents were estimated from the polarization curves of Fig. 3 in the manner described previously. These estimated values of the limiting hydrogen evolution current are equivalent to the corrosion currents, i_{cor}, shown in Table 3 since corrosion is under cathodic control ($b_a \ll b_c \to \infty$). Table 2 compares the calculated current ratios obtained via Equations 25 and 26 with the directly measured values. It is clear that good agreement is achieved, confirming the essential validity of these simple relationships. Nevertheless, this is an unexpected conclusion in view of the significant surface coverage by the separators (> 80%, Table 1).

Table 3. Parameters derived from low current polarization and faradaic impedance data at or near the open circuit (corrosion) potential

Electrode–separator system	*Impedance data*					*Polarization data*					
	C_{dl} ($\mu F\,cm^{-2}$)	R_{ct} (Ωcm^2)	i_0 ($\mu A\,cm^{-2}$)	R_{dc} (Ωcm^2)	$i_{cor}^{R_{dc}}$ ($\mu A\,cm^{-2}$)	R_p (Ωcm^{-2})	$i_{cor}^{R_p}$ ($\mu A\,cm^{-2}$)	i_{cor}^{Ext} ($\mu A\,cm^{-2}$)	I_{cor} (%)	i_{cor}^{Bat} ($\mu A\,cm^{-2}$)	I_{cor}^{Bat} (%)
Zn	7.5	183	71	1850	7.5	2017	8.2	8.0	–	8.0	–
Zn–paper	16	230	57	850	9.5	1007	11.3	9.0	0	9.0	0
Zn(Hg)	20	107	122	–	–	2400	6.5	5.0	–	5.0	–
Zn(Hg)–separator B	45	300	43	–	–	2162	6.0	4.2	16	4.2	16
Zn(Hg)–separator C	13	650	20	–	–	2796	4.6	5.5	0	5.5	0
Zn(Hg)–separator D	58	509	26	–	–	1540	–	4.8	4	4.8	4

The above result is difficult to explain, although it is interesting to note that the limiting hydrogen evolution current shows a similar insensitivity to both zinc amalgamation level [4] and the presence of adsorbed organic molecules even at high coverages [12]. This latter phenomenon has also been noted previously [13]. These effects suggest that the important interfacial factor determining the current is the *geometrical* area of the electrode. Thus the total flux of protons arriving at the electrode is independent of the nature of the electrode material. It is also independent of the presence of adsorbed organic molecules since, even when strongly adsorbed, the latter are in rapid dynamic equilibrium with the bulk solution and must therefore provide potential sites for proton reduction in a time scale which is many orders of magnitude less than that required for slow reactant surface diffusion from one surface site to another. The apparent result is that all sites become active as far as the diffusing entity is concerned, irrespective of surface coverage. Separator materials, however, are immobilized on the electrode surface thus providing a *permanent* blocking action which prevents the observed effects being explained by the same mechanism. It is possible that some kind of flux channelling occurs which concentrates the flux within the separator pores relative to that in the absence of the separator. This would increase the current *density* on the uncovered parts of the electrode while at the same time maintaining the total current constant. Alternatively, it is possible that the phenomenon is peculiar to the proton and results from its high mobility and small size which permits it to penetrate the metal–separator contact points which are normally inaccessible to other more bulky ions. This hypothesis has been provided previously to explain the deficient inhibition of the hydrogen evolution reaction in NH_4Cl solutions in the presence of methylcellulose-coated separators [2]. These speculative suggestions, however, require further elucidation.

4.3. *Comparison of double layer capacities, exchange currents and corrosion rates*

Table 3 summarizes data derived from low-current measurements at or near the open circuit (corrosion) potential. Data in respect of impedance and polarization measurements are presented separately.

The double-layer capacity values, which were determined from the impedance semicircles of Figs 1, 3 and 4 as discussed previously [2], can be seen to vary significantly. For pure zinc the value is very low at 7.5 $\mu F\,cm^{-2}$ due to the presence of the oxide film. In the presence of the base paper alone the capacity more than doubles confirming partial removal of the film, probably as a result of the fall in local pH discussed earlier. On amalgamated zinc the capacity is 20 $\mu F\,cm^{-2}$ confirming that the oxide is less protective and/or thinner than that on pure zinc. Nevertheless, the capacity is still well below that expected for a film-free zinc surface, prepared in the manner described here, close to the corrosion potential, namely 40 $\mu F\,cm^{-2}$ [4, 14]. In the presence of separator B, however, the capacity rises appreciably to 45 $\mu F\,cm^{-2}$, slightly exceeding the expected value. The same applies to separator D where the value is 58 $\mu F\,cm^{-2}$. These results can be explained if it is assumed that the presence of these *coated* separators induce a sufficiently large surface pH fall to cause complete removal of the semi-conducting oxide. Acidic groups, which are certainly present in the case of separator B as a result of the Karaya Gum, may also contribute. It can be seen that this behaviour does not apply to separator C which is anomalous, the capacity remaining low at 13 $\mu F\,cm^{-2}$. However, the separator coating is probably low in acidic surface groups. Conspicuously, the present set of capacity data indicate that there is no overall capacity lowering resulting from any blocking effect of the separator materials. This feature is in agreement with the earlier studies [1, 2].

The charge transfer resistances were converted to exchange currents using the expression defined previously (Equation 21). The values are, in general, several orders of magnitude less than those obtained, for example in standard Leclanché electrolyte [1], reflecting the very much lower zinc ion concentration in equilibrium with the electrode. The variation in i_0 from one electrode–separator system to another is complex, being affected by the oxide film and amalgamation level in addition to the nature of the particular separator present.

Data on the right hand side of Table 3 concerns the corrosion rate of zinc. It is important to note that no original information concerning the mechanism of action of the separator is possible by further analysis, since the net corrosion rate is determined by the juxtaposition of the individual anodic and cathodic polarization lines which have already been analysed and discussed. Nevertheless, it is important to quantify the overall effects, particularly those pertinent to the battery environment.

The corrosion currents tabulated were derived from the limit of the impedance at zero frequency by extrapolation (R_{dc}) using Equation 22; the polarization resistance (R_p) using Equation 22; and the extrapolation of polarization lines to the corrosion potential. The respective corrosion currents are $i_{cor}^{R_{dc}}$, $i_{cor}^{R_p}$ and i_{cor}^{Ext}. Values of $i_{cor}^{R_{dc}}$ for Zn(Hg) were inaccessible due to the fact that no significant *collapse* of the Warburg impedance to the resistive axis occurred even at the lowest frequencies. In general it can be seen that there is good agreement between the various methods of analysis proving their internal consistency. Using the i_{cor} values, corrosion inhibition factors, I_{cor}, were derived using the relationship

$$I_{cor} = 100[1 - (i_{cor}^{s}/i_{cor})] \tag{27}$$

where i_{cor}^{s} and i_{cor} are the corrosion currents in the presence and absence of the separator, respectively. In general the values are zero except for separators B and D. However, the corrosion inhibition afforded is minimal. This situation contrasts appreciably with that in NH_4Cl electrolyte where inhibition factors for the base paper and methylcellulose-coated paper separators of 40–74% were observed. The cause of the low inhibition efficiency is the diffusion-limited nature of the cathodic hydrogen evolution process which is not affected by the blocking action of the separators. This can be shown as follows. Since corrosion occurs under cathodic control, Equation 23 can be replaced by

$$I_{cor} = 100[1 - (i_c^{s}/i_c)] \tag{28}$$

Substitution of Equation 19 leads to

$$I_{cor} = 100[1 - A_e(\delta/l)] \tag{29}$$

But $A_e = 1$ and hence

$$I_{cor} = 100[1 - (\delta/l)] = 100[1 - (\delta/\theta t)] \tag{30}$$

In the present work $\delta \approx l$ and substitution in Equation 30 gives $I_{cor} \approx 0$.

There is one further consequence of the diffusion-limited nature of the corrosion rate-controlling cathodic process. To a first approximation the corrosion currents estimated in Table 3 for the analogue NaCl electrolyte will also pertain in the complete $ZnCl_2$ battery electrolyte. This is because the shift in corrosion potential produced by addition of Zn(II) ions will have little effect on i_{cor} ($b_c \approx \infty$). As a result, the corrosion inhibition factors will also be unaffected, as shown in Table 3. This situation again contrasts with that in NH_4Cl electrolyte where inhibition factors estimated for the complete battery electrolyte were roughly half those determined in the electrolyte analogue [2].

5. Conclusions

1. The polarization and impedance characteristics of amalgamated zinc immersed in flooded 2.7 M NaCl at pH 4.8, either in the presence or absence of separator materials, can be interpreted if due consideration is given to diffusion and charge transfer effects. The anodic zinc dissolution process is jointly controlled by these effects whereas the cathodic hydrogen evolution process is diffusion-limited.

2. Using a simple model which takes into account the quasi-reversible nature of the zinc dissolution process, good agreement between calculated and observed current inhibition factors can be

obtained if the surface blocking (coverage) effect of the separator is combined with the effect of the change in diffusion path length through the separator pores.

3. Application of the above model to diffusion-limited proton reduction fails unless the blocking term is ignored. However, if this is done then good agreement between the calculated and observed current ratios is once again achieved. It is tentatively suggested that either some kind of flux channelling within the separator pores increases the current density on the uncovered parts of the electrode surface, or the protons are freely able to gain access to those parts of the metal surface normally inaccessible to other bulkier ions.

4. The diffusion-limited nature of the hydrogen evolution process and accompanying lack of separator blocking ability leads to very low corrosion inhibiting efficiencies for the investigated separator materials in the NaCl analogue electrolyte. This situation is also expected to pertain in the complete $ZnCl_2$ battery electrolyte.

Acknowledgement

The authors wish to thank the Directors of British Ever Ready Ltd for permission to publish this work.

References

[1] L. M. Baugh and N. C. White, paper presented at 15th International Power Sources Symposium, Brighton, UK, September, 1986.
[2] L. M. Baugh and N. C. White, *J. Appl. Electrochem.* **17** (1987) 165.
[3] *Idem, ibid.* **17** (1987) 174.
[4] L. M. Baugh, F. L. Tye and N. C. White, *ibid.* **13** (1983) 623.
[5] R. D. Armstrong and G. M. Bulman, *J. Electroanal. Chem.* **25** (1970) 121.
[6] L. M. Baugh and A. R. Baikie, *Electrochim. Acta.* **30** (1985) 1173.
[7] L. M. Baugh, *Electrochim. Acta* **24** (1979) 657.
[8] F. L. Tye, *Chem. and Ind.* May (1982) 322.
[9] B. Poussard, V. Dechenaux, P. Croissant and A. Hardy, in J. Thomson (ed.) Power Sources 7, Academic Press, London, 1979, p. 445.
[10] J. A. Lee, W. C. Maskell and F. L. Tye, in P. Meares, (ed.), Membrane Separation Processes, Elsevier, Amsterdam, Ch. 11, p. 425.
[11] A. Agopsowicz, R. Brett, J. E. A. Shaw and F. L. Tye in D. H. Collins, (ed) Power Sources 5, Academic Press, London, p. 503.
[12] L. M. Baugh and J. A. Lee, *J. Electroanal. Chem.* **48** (1973) 63.
[13] R. Parsons in Surface Science, Vol. 2, Int. Atom. Energy Agency, Vienna, 1975, p. 144.
[14] L. M. Baugh, F. L. Tye and N. C. White, in J. Thomson (ed.), Power Sources 9, Academic Press, London, 1983, p. 303.